Hindawi
Geofluids
Volume 2021, Article ID 1401051, 8 pages
https://doi.org/10.1155/2021/1401051

Research Article

Fine Depiction of the Single Sand Body and Connectivity Unit of a Deltaic Front Underwater Distributary Channel: Taking the Third Member of the Dongying Formation in the Cha71 Fault Block of the Chaheji Oilfield as an Example

Zhenfeng Yu,[1,2,3] **Jindong Yang**,[3] **Xinya Song**,[3] **and Jin Qiao**[3]

[1]*Jinneng Holding Technology Center of Shanxi Science and Technology Research Institute (Jinneng), Jincheng 048000, China*
[2]*State Key Laboratory of Coal and CBM Co.-Mining, Jincheng 048000, China*
[3]*Shanxi Lanyan Coalbed Methane Engineering Research Co. Ltd., Jincheng 048000, China*

Correspondence should be addressed to Zhenfeng Yu; yzf1234560604@163.com

Received 4 June 2021; Revised 24 July 2021; Accepted 11 August 2021; Published 26 August 2021

Academic Editor: Xudong Zhang

By taking the third member of the Dongying Formation in the Cha71 fault block of the Chaheji oilfield as an example, the single sand body of the deltaic front underwater distributary channel is meticulously depicted by using the data of well logging and performance production. Portrays the vertical separation model, total lateral separation type, vertical type, lateral superposition type, 4 types of single sand body vertical superimposed and bay type, bank contact between docking, instead of four kinds of single sand body lateral contact type, and summarizes its logging facies identification. The quantitative prediction model of the single sand body was established, the characteristics of single sand body plane distribution were summarized, and the identification of the oil-water layer and the lower limit of reservoir effective thickness were studied. And we got the conclusion that based on the fine characterization of the single sand body and the lower limit standard of effective reservoir thickness, the distribution range of the effective reservoir and connecting unit is determined. Finally, the connectivity of the connecting unit is verified by dynamic data.

1. Introduction

At present, most of the old oilfields in eastern China have entered the stage of high water cut after several rounds of water injection development. The distribution of remaining oil is very complex and presents a highly isolated state. Therefore, the conventional research on a small layer-level reservoir cannot meet the production needs. It is urgent to carry out the research on a single sand body-level reservoir [1–7]. A single sand body refers to its own vertical and horizontal continuous distribution, but it is different from the upper and lower sand bodies. A sand body with mudstone or an impermeable interlayer is the smallest reservoir unit and the coarser unit with similar lithology and attributes in the sedimentary rhythm [8–11]. In this study, taking the east third member of the Cha71 fault block in the Chaheji oilfield as an example, the contact type of the single sand body in the study area is accurately identified by comprehensive utilization of logging and production performance data, and the identification marks of logging facies are summarized. The quantitative prediction model of the single sand body is established, the plane distribution characteristics of the single sand body are summarized, the identification of oil and water layers and the lower limit of effective thickness of the reservoir are carried out, the distribution range of the effective reservoir and connected unit is determined, and the connectivity of the connected unit is verified by dynamic data.

The Cha71 fault block in the Chaheji oilfield is located in Baxian County, Langfang City, Hebei Province, belong-

ing to the tertiary oilfield in the Jizhong exploration area [12]. The structure is located in the middle of the eastern sag of the Jizhong depression, adjacent to the Niutuozhen uplift in the west and the Baxian trough [13–17] in the east. Five nearly east-west normal faults are developed, which cut each other and have a complex relationship, and the five faults run through the east 2 member, east 3 member, and upper Sha 1 member from top to bottom, belonging to the complex fault block reservoir under the common control of structure and lithology [18]. At present, the main target layer of the study area is the third member of the east formation, with an area of about 6.27 km^2, a total of 144 wells, including 113 oil production wells and 31 water injection wells. There are 4 oil formations I, II, III, and IV and 38 small layers. The lithology of the reservoir is mainly argillaceous siltstone, with the main particle size of 0.2-0.8 mm; the porosity is mainly distributed in 8%-20%, with the highest peak of 12%, with an average of 15.3%; the permeability is mainly distributed in $0.1 \times 10^{-3}\,\mu m^2$ -$100 \times 10^{-3}\,\mu m^2$, with the highest peak of $0.1 \times 10^{-3}\,\mu m^2$ -$1 \times 10^{-3}\,\mu m^2$, with an average of $2 \times 10^{-3}\,\mu m^2$. The reservoir belongs to the low-porosity and low-permeability reservoir.

2. Materials and Methods

2.1. Fine Description of the Single Sand Body

2.1.1. Contact Type and Identification Mark of the Single Sand Body. During the rise and fall of the lake level, the ratio of the accommodation space to the sediment supply rate will change constantly [19, 20], so the preservation degree and contact pattern of the single sand body will change constantly. Based on the fine dissection of the dense well pattern in the study area of the third member of the east of the Cha71 fault block in the Chaheji oilfield, four types of the single sand body longitudinal superimposition, namely, vertical separation type, lateral separation type, vertical superposition type, and lateral superposition type, and four types of single sand body transverse contact, namely, interbay contact type, dike contact type, butt joint type, and substitution type, are identified, and the logging acquaintance of different superimposed sand bodies (contact type) is summarized.

(1) Types and Identification Marks of the Single Sand Body Superimposed Vertically.

(1) Vertical separation type

The vertical separation type refers to the vertical superposition of two single sand bodies, but due to the existence of argillaceous intercalation, the two single sand bodies are not connected vertically and have independent pressure and seepage systems. The spontaneous potential and induced conductivity curves show two distinct bell-shaped and box-shaped characteristics, and the muddy interlayer shows obvious return characteristics.

(2) Lateral separation type

The lateral separation type refers to the lateral superposition of two single sand bodies, but due to the existence of the argillaceous interlayer, the two single sand bodies are not connected longitudinally, and each has its own pressure and seepage system. The spontaneous potential and induced conductivity curves show two distinct box types in the superimposed area, a single box type in the nonsuperimposed area, and obvious return characteristics in the muddy interlayer.

(3) Vertical superimposed type

The vertical superimposed type refers to that the two-stage single sand bodies are vertically superimposed and connected, the late stage single sand body has a weak degree of erosion transformation to the early stage single sand body, and the two-stage single sand bodies have a unified pressure and seepage system. The spontaneous potential and induced conductivity curves show two obvious stepped box shapes in the superimposed area of two single sand bodies.

(4) Lateral superimposed type

The lateral superimposed type refers to that the two-stage single sand bodies are laterally superimposed and connected, the late single sand bodies have no obvious erosion transformation to the early single sand bodies, and the two-stage single sand bodies have a unified pressure and seepage system. The spontaneous potential and induced conductivity curves show two obvious stepped box and bell shapes in the superimposed area of the two single sand bodies and a single box shape in the nonsuperimposed area.

(2) Types and Identification Marks of Single Sand Body Lateral Contact.

(1) Interbay contact type

The interbay contact type refers to the development of underwater distributary interbay argillaceous deposits between two single sand bodies in the same sedimentary period. The two single sand bodies are not connected laterally and have independent pressure and seepage systems. The spontaneous potential and induced conductivity curves show a box and bell type at the two single sand bodies and a flat type at the muddy sediments of the underwater distributary bay.

(2) Bank contact type

The bank contact type refers to the underwater natural dike developed between two single sand bodies in the same sedimentary period. Because the main composition of the underwater natural dike is siltstone or argillaceous siltstone, the two single sand bodies are not connected horizontally, and each has its own pressure and seepage system. The

spontaneous potential and induced conductivity curves show a box shape at the two single sand bodies and a saw tooth shape at the underwater natural dike.

(3) Butting type

Butting type refers to that two single sand bodies in the same sedimentary period are butted with each other, the degree of erosion and transformation between the two single sand bodies is weak, the single sand bodies are laterally disconnected or weakly connected, and the profile shape of single sand bodies presents the characteristics of thick thin thick. The spontaneous potential and induced conductivity curves show an isolated box shape at the two single sand bodies, but the amplitude of the box shape is different.

(4) Substitute type

The substitute type refers to the mutual erosion and transformation between two single sand bodies in the same sedimentary period, the single sand bodies are connected horizontally, and the two single sand bodies have a unified pressure and seepage system. The spontaneous potential and induced conductivity curves show an isolated box shape at the two single sand bodies, but the amplitude of the box shape is different.

2.1.2. Quantitative Prediction Model of the Single Sand Body. In order to quantitatively predict the distribution range of the single sand body in the area with few wells or no wells, count the width and thickness of different single sand bodies in the dense well pattern area of oil groups I, II, III, and IV in the third member of East China, establish the quantitative interpretation model of the width thickness ratio of the single sand body in oil groups I, II, III, and IV (Figure 1), and predict the transverse distribution range of the single sand body in the area with few wells or no wells through the interpretation model of the width thickness ratio 2 : 1 of the single sand body [21].

2.1.3. Plane Distribution Characteristics of the Single Sand Body. On the basis of fine dissection of the dense well pattern, combined with the interpretation model of the width thickness ratio of the single sand body, the plane distribution characteristics of the single sand body are studied. Taking the 6 small layers of east member III oil formation as an example, 8 stages of single sand bodies are finely identified in this small layer horizontally, among which 1, 2, 3, and 4 single sand bodies belong to no. 6_1 single sand layer and no. 5, no. 6, and no. 7 single sand bodies belong to the no. 6_2 single sand layer; most of the single sand bodies are delta front underwater distributary channel sand bodies, and a few are far bar sand bodies. The single sand bodies extend from northwest to southeast in a strip and gradually bifurcate, indicating that the provenance is the northwest direction, and there are vertical superposition and horizontal contact during the development of single sand bodies. The overlapping parts of no. 1 and no. 5, no. 2 and no. 6, and no. 3 and no. 6 single sand bodies present a vertical superposition type, the overlapping parts of no. 2 and no. 5 single sand bodies present a lateral superposition type, the overlapping parts of no. 4 and no. 6 single sand bodies present both the vertical superposition type and lateral superposition type, and the transverse contact parts of no. 2 and no. 3 single sand bodies present a butt joint type. According to the statistics of the width and thickness of the single sand body in 8 stages of 6 layers in the third member of east member III oil formation, the maximum width of the single sand body is 421 m and the minimum is 47 m and the maximum thickness is 4.7 m and the minimum is 0.8 m.

2.2. Identification of Oil and Water Layers and Determination of Effective Thickness. At present, the methods of oil-water layer identification mainly include a microdifference map method, no invasion line method, and crossplot method [22]. The crossplot method is to use the original logging information or calculation information to form a crossplot. According to the distribution law of data points in the crossplot, the oil layer and water layer can be distinguished [23]. Because the crossplot method is fast, direct, and easy to operate and can correctly identify the properties of most reservoir fluids [24], the crossplot technology is one of the most effective qualitative and semiquantitative reservoir identification technologies in logging evaluation for the single sand body [25].

2.2.1. Classification Standard of Correction Test Results. According to the analysis of production test results of coring wells (Table 1), well C71-69 has a depth of 2367.0-2371.2 m and a water cut of 24.34%, indicating that it is an oil layer; well C15-322 has a depth of 2181.8-2184.4 m and a water cut of 1.52%, indicating that oil and water are in the same layer.

According to the statistics of acoustic transit time and induced conductivity curve values of coring wells in the study area, through the crossplot of acoustic transit time and induced conductivity (Figure 2), it can be analyzed that the data points of the oil layer, oil-water layer, oil-water layer, and water layer are mixed. Based on the test results and crossplot, it is difficult to identify oil and water layers quickly and accurately, so it is necessary to correct the test results.

2.2.2. Establishment of Quantitative Identification Standard for Oil and Water Layers. According to the latest oil-water layer classification standard and combined with the actual situation of production data in the study area, a set of oil test conclusion classification standards in line with the region are formulated: water cut < 25% is judged as an oil layer, 25% ≤ water cut ≤ 75% is judged as an oil-water layer, 75% < water cut < 100% is judged as an oil-bearing layer, and water cut = 100% is judged as a water layer. The oil and water layers are identified by using the latest classification standard of well testing conclusion, and the natural potential, acoustic time difference, and induced conductivity of the well testing layer are counted. It can be seen that if COND is less than 175 mS/m, it is mainly an oil testing layer and the same layer; if COND is more than 175 mS/m, it is mainly an oil testing water layer and oil-bearing water layer.

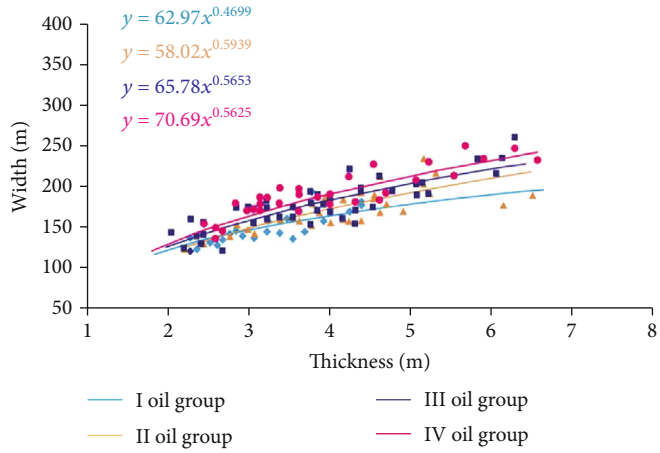

Figure 1: Width thickness ratio of the single sand body in the east third section of the Cha71 fault block in the Chaheji oilfield.

Table 1: Oil testing conclusion of the third member of the east Cha71 fault block in the Chaheji oilfield.

Well	Interval	Top depth (m)	Bottom depth (m)	Lithology	Accum. oil production (t)	Accum. water production (t)	Water cut (%)	Conclusion
C71-69	Dongsan	2367.0	2371.2	Sand	20.20	6.50	24.34	Oil layer
C15-322	Dongsan	2181.8	2184.4	Sand	162.00	2.50	1.52	Oil and water layer

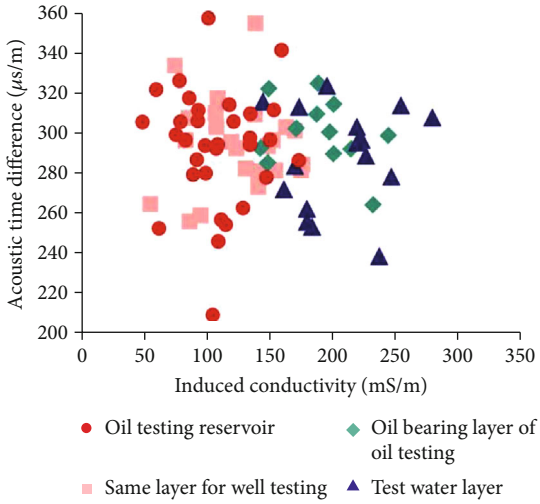

Figure 2: Crossplot of acoustic time difference and induced conductivity in the third member of the east of the Cha71 fault block in the Chaheji oilfield.

The 175 mS/m boundary can well separate the test oil layer from the test water layer, and the resistivity value corresponding to the 175 mS/m induced conductivity is 5.7 Ω m (Figures 3 and 4).

2.2.3. Determine the Lower Limit of Effective Thickness. According to the regulations of the code for the calculation of oil and gas reserves, the effective thickness refers to the thickness of the part of the reservoir with oil production capacity in the oil- and gas-bearing series that meets the reserve calculation standard [26]. In the new guide to calculation of oil and gas reserves, the requirements for effective thickness have been improved, and it is further clarified that effective thickness refers to the thickness of the reservoir with oil and gas production capacity in the oil- and gas-bearing strata that meet the reserve calculation standard [27]. At present, the main methods to determine the lower limit of effective thickness include the empirical statistical method, mercury injection parameter method, testing method, oil bearing occurrence method, permeability stress sensitivity method, and porosity permeability crossplot method [28, 29]. The crossplot method is adopted in this study.

Lithology lower limit: the lithology of the reservoir in the third member of the east is mainly argillaceous siltstone, siltstone, argillaceous fine sandstone, and fine sandstone (Figure 5). Through thin section data, grain size analysis data, oil-bearing grade judgment, and comprehensive lithology statistics, it is concluded that the oil-bearing rock type is mainly argillaceous siltstone, so the lithology lower limit of the reservoir in the third member of the east is argillaceous siltstone.

Lower limit of physical property: through the analysis of core physical property and oil-bearing property of the Dongsan member coring well, it can be concluded that there is an obvious boundary between oil trace and reservoir physical property of oil grade above oil trace and below oil trace, which is the lower limit of porosity and permeability, with porosity of 17% and permeability of $20 \times 10^{-3}\ \mu m^2$, respectively (Figure 6).

Lower limit of electrical property and lower limit of oil-bearing property: according to the oil testing, logging, and coring data in the study area, crossplot of reservoir acoustic

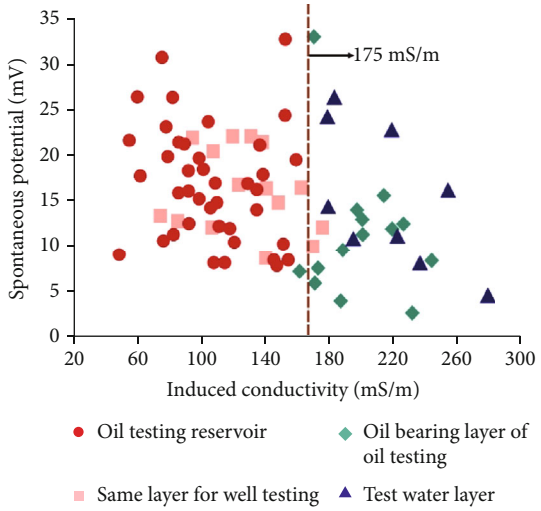

Figure 3: Crossplot of spontaneous potential and induced conductivity, crossplot of spontaneous potential, acoustic time difference, and induced conductivity in the third member of the east Cha71 fault block, Chaheji oilfield.

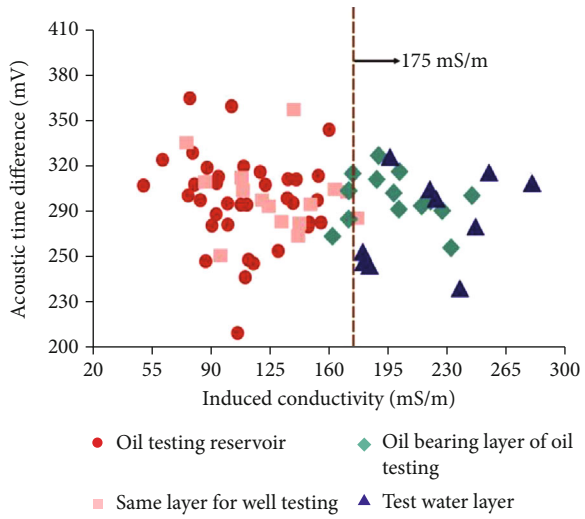

Figure 4: Crossplot of acoustic transit time and induced conductivity, crossplot of spontaneous potential, acoustic time difference, and induced conductivity in the third member of the east Cha71 fault block, Chaheji.

time difference and formation resistivity is drawn (Figure 7). Formation resistivity can well reflect oil-bearing property, and the crossplot of resistivity acoustic time difference can be used to judge the oil layer, oil-water layer, oil-water layer, tight layer, and water layer. Therefore, the lower limit of electrical property of the same layer is 5.7 Ω m and 253 μs/m.

3. Results and Discussion

3.1. Static Characterization of Connected Elements. According to the lower limit standard of effective thickness, fault, structure, and other control factors, we study the no. 1 single

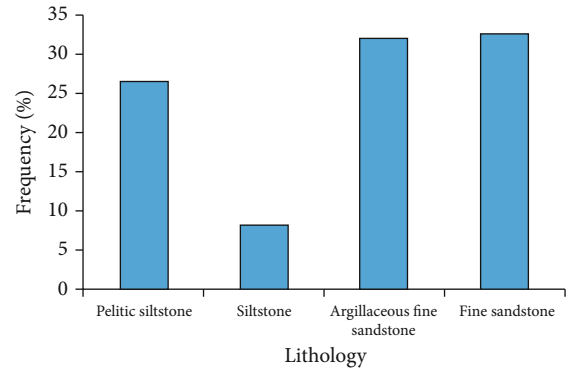

Figure 5: Crossplot of spontaneous potential and induced conductivity in the third east member of the Cha71 fault block in the Chaheji oilfield.

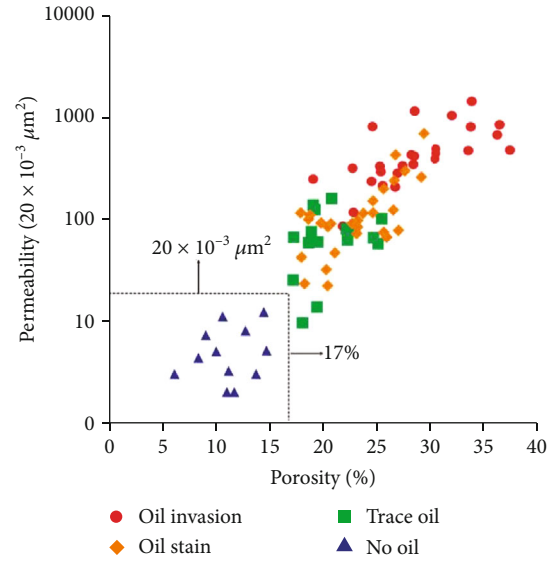

Figure 6: Lower limit of porosity permeability of the east third section of the Cha71 block in the Chaheji oilfield.

sand body in the 6-layer 6_1 single sand body and no. 5 single sand body in the 6_2 single sand body, five boundary types are identified, and the oil-water interface of the effective reservoir is -2180 m according to the lower limit standard of the oil-water layer, which is the boundary of the oil-water interface; according to the lower limit standard of lithology, the lithologic boundary of the effective reservoir is identified; according to the control effect of structure on the effective reservoir, the effective reservoir is identified. The reservoir is a lithologic updip monoclinic reservoir; the lithologic updip direction is the fault boundary; according to the physical property lower limit standard and oil-water layer identification standard, the poor physical property is the physical property boundary. Finally, the oil-bearing areas of the effective reservoirs delineated by the five kinds of boundaries are 0.197 km^2 and 0.206 km^2, respectively.

The laterally superimposed connecting unit of the third member of the east is composed of C71-82, C71-79, and

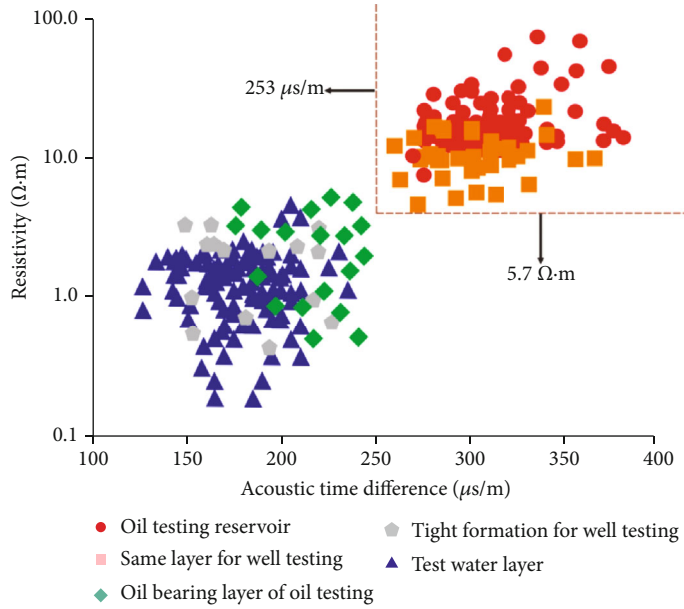

Figure 7: Crossplot of formation resistivity and acoustic time difference in the third member of the east Cha71 fault block in the Chaheji oilfield.

C71-85 wells in the 6_1 single sand layer, 1 single sand body, and 6_2 single sand body, and the effective reservoir of the no. 5 single sand body of the no. 2 single sand layer is vertically superimposed. According to the profile of the connected unit, it can be concluded that there is 6 in well C71-82 6_1 single sand layer, 1 single sand body, and 6_2 single sand body; the effective reservoir of the no. 5 single sand body of the no. 2 single sand layer is connected vertically, with a 3 m thick poor oil layer at the bottom and a 1.4 m thick oil layer at the upper part. In C71-79 well zhong 6_1, the effective reservoir of the no. 1 single sand body of the No. 1 single sand layer is a 2 m thick poor oil layer. In the C71-85 well 6_2 layer, the effective reservoir of the no. 5 single sand body in the no. 2 single sand layer is 1.4 m thick oil layer, and the oil-bearing area of the lateral superimposed connected unit is 0.33501 km^2.

3.2. Dynamic Test of the Connected Unit. In order to test the connectivity of the static characterization connected unit, the tracer technology is used to dynamically verify the connectivity of the static characterization connected unit. Taking well groups C71-85, C71-82, and C71-79 as examples, well C71-82 injects 500 ml tracer with a depth of 2133.4-2728.4 m. Through monitoring the surrounding wells, the tracer is detected in well C71-79 223 m away from well c71-82 after 105 days, and in well C71-8 223 m away from well C71-82 after 128 days, the trace is detected in well C71-85 159 m away from well C71-85. The water absorption profile of well C71-82 shows that the water absorption intensity of layer 35 of the well is relatively high. Through the analysis of the lateral superimposed connecting unit of oil group III of the Dongsan Formation, layer 35 of well C71-82 corresponds to the 6-1 single sand layer, and the single sand layer is perforated. The 6-1 single sand layer of well C71-79 and the 6-2 single sand layer of well C71-85 are perforated. Therefore, the trace enters the connecting unit from the 6-1 single sand layer of well C71-82 and flows to the two sides along the provenance direction, the tracer source of well C71-79 is a 6-1 single sand layer, and the diffusion rate is 2.12 m/d; against the provenance direction, the tracer source of well C71-85 is the 6-2 single sand layer, and the diffusion rate is 1.24 m/d (Table 2). Therefore, the lateral superimposed connected unit is connected vertically.

Table 2: Effective corresponding table of the well group C71-82 in the third east member of the Cha71 fault block in the Chaheji oilfield.

Well	C71-79	C71-85
Well distance	223 m	159 m
Day	105 d	128 d
Diffusion rate	2.12 m/d	1.24 m/d

4. Conclusions

(1) Through fine description of single sand bodies in four oil formation dense well pattern areas in the third member of the East China Sea, four types of single sand bodies are identified: vertical separation type, lateral separation type, vertical superimposed type, and lateral superimposed type, and four types of single sand bodies are identified: interbay contact type, bank contact type, butting type, and substitute type. The prediction model of the single sand body

width thickness ratio of four oil formations in the study area is established

(2) The quantitative identification standard of the oil-water layer in the third member of the East China Sea is established: the oil layer and oil-water layer are the same when the induced conductivity is less than 175 mS/m, and the water layer and oil-bearing layer are the same when the induced conductivity is greater than 175 mS/m. The lower limit of lithology determined by effective thickness is argillaceous siltstone, the lower limit of physical property is porosity 17%, the permeability is $20 \times 10^{-3}\ \mu m^2$, the lower limit of electrical property and oil-bearing property is resistivity 5.7 Ω m, and the acoustic time difference is 253 μs/m

(3) Based on the fine description of the single sand body and the study of the lower limit of effective thickness of the reservoir, the laterally superimposed connected unit is statically characterized, which consists of the 6_1 single sand layer, 1 single sand body, and 6_2 single sand body; the effective reservoir of the no. 5 single sand body of the no. 2 single sand layer is formed laterally, with an oil-bearing area of 0.33501 km^2. At the same time, the tracer technology is used to dynamically test the connected unit, and the results show that the connected unit is connected vertically

Data Availability

All data included in this study are available upon request by contact with the corresponding author.

Conflicts of Interest

The authors declare no conflict of interest.

Acknowledgments

We gratefully acknowledge the Jinneng Holding Technology Center of Shanxi Science and Technology Research Institute (Jinneng), State Key Laboratory of Coal and CBM Co.-Mining, Shanxi Lanyan Coalbed Methane Engineering Research Co. Ltd., National Natural Science Foundation of China (41774126), and National Science and Technology Major Project of China (2016ZX05024-001, 2016ZX05006-002) for the financial support.

References

[1] D. Fang, J. Qian, and G. Jingjing, "Quantitative description of remaining oil based on single sand body of fan delta reservoir: a case study of ES in North Liuzan oilfield, Nanpu Sag_3 ~ 3 reservoir as an example," *Fault Block Oil and Gas Fields*, vol. 24, no. 4, pp. 529–535, 2017.

[2] F. Congjun, Z. Bao, and D. Chunming, "Superimposition mechanism of single sand body in underwater distributary channel of delta front and its control on remaining oil: a case study of the fourth member of Quantou Formation in block J19 of Fuyu oilfield," *Petroleum and Natural Gas Geology*, vol. 36, no. 1, pp. 128–135, 2015.

[3] F. Congjun, Z. Bao, and D. Qitong, "Division of single sand body in composite distributary channel of delta plain: a case study of the fourth member of Quantou Formation in the south of central Fuyu oilfield," *Petroleum and Natural Gas Geology*, vol. 33, no. 1, pp. 77–83, 2012.

[4] Z. Li, Z. Bao, and Y. Lin, "Sand body types and sedimentary models of shallow water delta: a case study of the first member of Cretaceous Yaojia Formation in Qian'an area, southern Songliao Basin," *Petroleum Exploration and Development*, vol. 44, no. 5, pp. 727–736, 2017.

[5] M. Shizhong, L. Guiyou, Y. Baiquan, and F. Guangjuan, "Study on "three dimensional heterogeneity model controlled by building structure" of channel single sand body," *Geoscience frontier*, vol. 1, pp. 57–64, 2008.

[6] N. Bo, Z. Jiahong, and Z. Bao, "Determination of abandoned meandering river channel strike and characterization of single sand body configuration: a case study of the lower member of Neogene Minghuazhen Formation in the west of Shijiutuo uplift, Chengning uplift, Bohai Bay Basin," *Petroleum Exploration and Development*, vol. 46, no. 5, pp. 891–901, 2019.

[7] W. Jue, X. X. Jun, and Z. Xinmao, "Structural characterization and remaining oil distribution pattern of meandering river Dianba reservoir," *Journal of China University of Petroleum (NATURAL SCIENCE EDITION)*, vol. 43, no. 3, pp. 13–24, 2019.

[8] X. Yu, "Reservoir problems in the middle and late stage of oilfield development and geological characterization method based on sedimentary genesis," *Geoscience Frontier*, vol. 19, no. 2, pp. 1–14, 2012.

[9] Z. Yupan, "Fine description of composite underwater distributary channel sand bodies in Chang 8, Jihuang 32 block_1 ~ 1 reservoir development," *China Mining*, vol. 29, Supplement 1, pp. 436–440 + 444, 2020.

[10] L. Xingguo, *Sedimentary Microfacies and Microstructure of Continental Reservoirs*, Petroleum Industry Press, Beijing, 2000.

[11] X. Hui, L. Chengyan, and L. Guanglun, "Distribution of residual oil in single sand body of underwater distributary channel and countermeasures for tapping potential," *Journal of China University of Petroleum (NATURAL SCIENCE EDITION)*, vol. 37, no. 2, pp. 14–20 + 35, 2013.

[12] L. Huaiyu, Z. Weihong, and W. Lianjun, "Discovery of turbidite in Chaxi area and its significance for oil and gas exploration," *Acta Sedimentologica Sinica*, vol. 26, no. 1, pp. 89–94, 1999.

[13] J. Yang, Z. Yiping, and A. Wang, "Beach bar sedimentary characteristics of the upper Es3 member in Gaojiapu area of Baxian sag," *Special Oil and Gas Reservoirs*, vol. 24, no. 1, pp. 1–5, 2017.

[14] L. Chuanbing, C. Tongran, and Z. Feng, "Sedimentary characteristics of shallow water delta and its significance for oil and gas exploration: a case study of upper SHA-1 member of Chaheji structural belt, Baxian sag, Bohai Bay Basin," *Xinjiang Petroleum Geology*, vol. 37, no. 6, pp. 625–630, 2016.

[15] Z. Yanan, *Study on Sedimentary Facies of the East Third Member of Chaheji Structural Belt*, Southwest Petroleum University, 2015.

[16] W. Quan, W. Daojun, and Z. Huayao, "Biomarker characteristics of Paleogene source rocks and their contribution to

hydrocarbon accumulation in Baxian sag," *Petroleum Geology and Recovery*, vol. 24, no. 6, pp. 17–24, 2017.

[17] Z. Wei, *Study on the Migration and Distribution of Oil and Gas in Chaheji Oilfield*, China University of Geology (Beijing), 2016.

[18] C. Yuqiu, *Sedimentary Characteristics and Prediction of Favorable Reservoir Facies of Shahejie Formation in Chaheji Oilfield*, Yanshan University, 2018.

[19] R. Shuangpo, Y. Guangqing, and M. Wenjing, "Genetic types and superimposition model of thin single sandbodies in underwater distributary channel of delta front: a case study of member IV - VI oil formation of he 3 in Biqian 10 area of Gucheng oilfield," *Acta Sedimentologica Sinica*, vol. 34, no. 3, pp. 582–593, 2016.

[20] H. Guangyi, C. Fei, and F. Tingen, "Subdivision and correlation method of fluvial facies reservoir based on composite sandbody configuration style," *Daqing Petroleum Geology and Development*, vol. 36, no. 2, pp. 12–18, 2017.

[21] H. Lei, S. Pingping, and S. Xinmin, "Oil water layer identification and reservoir type evaluation of low permeability oilfield," *Petroleum Exploration and Development*, vol. 48, no. 2, pp. 49-50, 2003.

[22] C. Gang, "A new crossplot for identifying low resistivity reservoirs and its application," *Journal of China University of Petroleum (NATURAL SCIENCE EDITION)*, vol. 52, no. 3, pp. 36–39, 2008.

[23] Tanyandong, *The Best Interpretation of Logging Data*, Geophysical anthology, 1983.

[24] Z. Ying, Y. L. Li, and C. M. Yin, "Identification of low resistivity reservoirs in Yan'an Formation in Zhenbei area by array induction invasion factor method combined with acoustic resistivity crossplot," *Journal of Xi'an University of Petroleum (NATURAL SCIENCE EDITION)*, vol. 29, no. 3, pp. 8–14 + 6, 2014.

[25] L. Shi'an and G. Min, *Comprehensive Interpretation of Logging Data*, Petroleum Industry Press, Beijing, 2002.

[26] Y. Tongyou and F. Shangjiong, *Calculation Method of Oil and Gas Reserves*, Petroleum Industry Press, Beijing, 1990.

[27] X. Zhang, E. Zhai, Y. Wu, D.'. Sun, and Y. Lu, "Theoretical and numerical analyses on hydro–thermal–salt–mechanical interaction of unsaturated salinized soil subjected to typical unidirectional freezing process," *International Journal of Geomechanics*, vol. 21, no. 7, article 04021104, 2021.

[28] G. Rui, "Determination method of lower limit value of reservoir physical property and its supplement," *Petroleum Exploration and Development*, vol. 44, no. 5, pp. 140–144, 2004.

[29] C. Y. Liu, Y. Wang, X. M. Hu, Y. L. Han, X. P. Zhang, and L. Z. Du, "Application of GA-BP neural network optimized by Grey Verhulst model around settlement prediction of foundation pit," *Geofluids*, vol. 2021, Article ID 5595277, 16 pages, 2021.